

# Nonlinear, Extended-Magnetohydrodynamic Modeling of Disruption Mitigation

by

**Brendan C. Lyons<sup>1</sup>,**

**J. McClenaghan<sup>1</sup>, C.C. Kim<sup>2</sup>, S.C. Jardin<sup>3</sup>, N.M. Ferraro<sup>3</sup>, C Akçay<sup>1</sup>,  
N.W. Eidietis<sup>1</sup>, L.L. Lao<sup>1</sup>, N. Hawkes<sup>4</sup>, G. Szepesi<sup>4</sup>, and JET contributors<sup>5</sup>**

<sup>1</sup> General Atomics

<sup>2</sup> SLS2 Consulting

<sup>3</sup> Princeton Plasma Physics Laboratory

<sup>4</sup> Culham Centre for Fusion Energy

<sup>5</sup> J. Mailloux, Nucl. Fusion (2022) <https://doi.org/10.1088/1741-4326/ac47b4>

Presented at the

**2022 Sherwood Fusion Theory Conference**

**Santa Rosa, California, USA**

**April 4<sup>th</sup>, 2022**

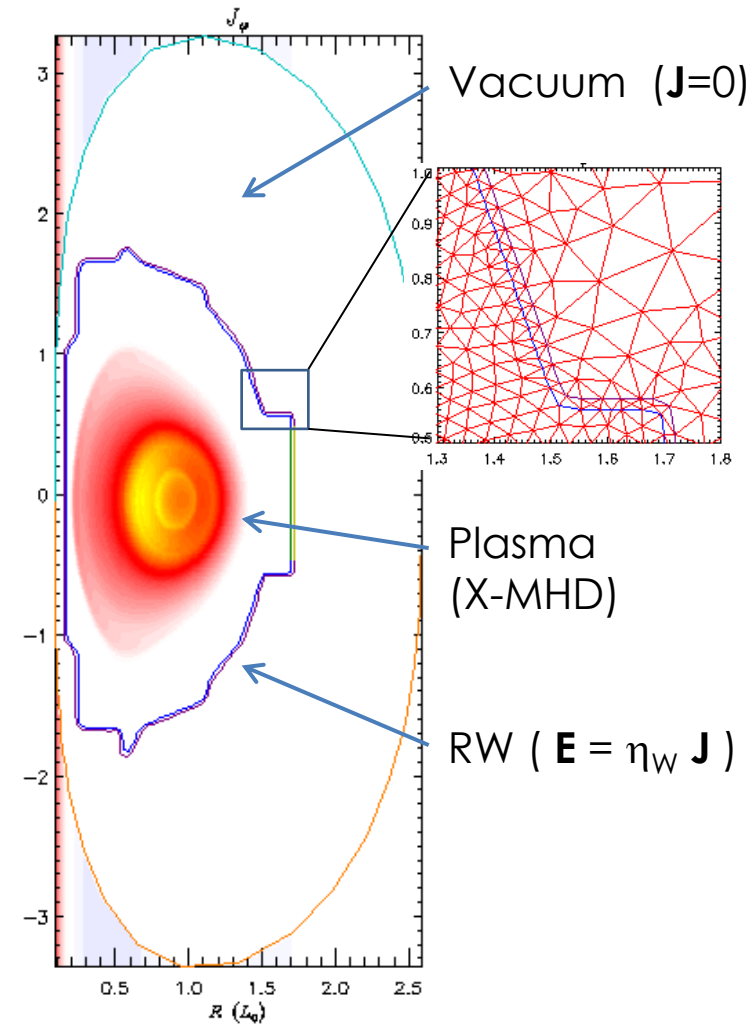
# Modeling of Disruption Dynamics and Mitigation Requires a Multiphysics Model

- **Disruptions pose a risk of damage to future tokamaks, necessitating robust mitigation techniques**
- **Most promising method uses pellet injection of impurities to radiate stored energy**
- **Simulations, validated against mitigation experiments, are required to project techniques to future devices**
- **Integrated model is required to capture all relevant physics**
  - Magnetohydrodynamics (MHD) for macroscopic evolution of disruption dynamics
  - Atomic physics for ionization and radiation from injected impurities
  - Drift-kinetics for phase-space evolution of runaway electron population

# M3D-C1 Code Overview

# M3D-C1\* Solves the Extended-MHD Equations

- Three-dimensional toroidal geometry
- Full (not reduced) MHD
- Solves for potential and stream-function fields for  $\vec{A}$  &  $\vec{v}$  ( $\nabla \cdot \vec{B} = 0$  intrinsically)
- Includes resistivity, density diffusivity, viscosity, & thermal conductivity
- Two-fluid effects (optional)
- 3D high-order finite elements
  - Unstructured, triangular mesh in poloidal plane
  - Structured toroidally, but can pack planes
- Can solve with finite-thickness resistive wall in domain\*\*



\*S. C. Jardin, et al., *Comput. Sci. Discovery* 5, 014002 (2012).

\*\*N.M. Ferraro, et al., *Phys Plasma* 23 056114 (2016).

# M3D-C1 Solves the Extended-MHD Equations

Blue terms are 2-fluid

$$\frac{\partial n}{\partial t} + \nabla \cdot (n\mathbf{V}) = \nabla \cdot D_n \nabla n + S_n$$

$$\frac{\partial \mathbf{A}}{\partial t} = -\mathbf{E} - \nabla \Phi, \quad \mathbf{B} = \nabla \times \mathbf{A}, \quad \mathbf{J} = \nabla \times \mathbf{B}, \quad \nabla_{\perp} \cdot \frac{1}{R^2} \nabla \Phi = -\nabla_{\perp} \cdot \frac{1}{R^2} \mathbf{E}$$

$$nM_i \left( \frac{\partial \mathbf{V}}{\partial t} + \mathbf{V} \cdot \nabla \mathbf{V} \right) + \nabla p = \mathbf{J} \times \mathbf{B} - \nabla \cdot \mathbf{\Pi}_i + \mathbf{S}_m$$

$$\mathbf{E} + \mathbf{V} \times \mathbf{B} = \frac{1}{ne} \left( \mathbf{R}_c + \mathbf{J} \times \mathbf{B} - \nabla p_e - \nabla \cdot \mathbf{\Pi}_e \right) - \frac{m_e}{e} \left( \frac{\partial \mathbf{V}_e}{\partial t} + \mathbf{V}_e \cdot \nabla \mathbf{V}_e \right) + \mathbf{S}_{CD}$$

$$\frac{3}{2} \left[ \frac{\partial p_e}{\partial t} + \nabla \cdot (p_e \mathbf{V}) \right] = -p_e \nabla \cdot \mathbf{V} + \frac{\mathbf{J}}{ne} \cdot \left[ \frac{3}{2} \nabla p_e - \frac{5}{2} \frac{p_e}{n} \nabla n + \mathbf{R}_c \right] + \nabla \cdot \left( \frac{\mathbf{J}}{ne} \right) : \mathbf{\Pi}_e - \nabla \cdot \mathbf{q}_e + Q_{\Delta} + S_{eE}$$

$$\frac{3}{2} \left[ \frac{\partial p_i}{\partial t} + \nabla \cdot (p_i \mathbf{V}) \right] = -p_i \nabla \cdot \mathbf{V} - \mathbf{\Pi}_i : \nabla \mathbf{V} - \nabla \cdot \mathbf{q}_i - Q_{\Delta} + S_{iE}$$

$$\mathbf{V}_e = \mathbf{V}_i - \mathbf{J} / ne$$

$$\mathbf{R}_c = \eta ne \mathbf{J}, \quad \mathbf{\Pi}_i = -\mu \left[ \nabla \mathbf{V} + \nabla \mathbf{V}^{\dagger} \right] - 2(\mu_c - \mu)(\nabla \cdot \mathbf{V}) \mathbf{I} + \mathbf{\Pi}_i^{GV}$$

$$\mathbf{q}_{e,i} = -\kappa_{e,i} \nabla T_{e,i} - \kappa_{\parallel} \nabla_{\parallel} T_{e,i}$$

$$\mathbf{\Pi}_e = (\mathbf{B} / B^2) \nabla \cdot \left[ \lambda_h \nabla (\mathbf{J} \cdot \mathbf{B} / B^2) \right], \quad Q_{\Delta} = 3m_e (p_i - p_e) / (M_i \tau_e)$$

# KPRAD\* Provides Needed Atomic Physics Information

- **KPRAD solves for impurity-plasma interaction in low-density, coronal model**
  - N.B. *not* coronal equilibrium
  - Based on ADPAK rate coefficients
  - Impurity charge states and electron density evolve according to ionization and recombination

$$\frac{\partial n_z}{\partial t} + \nabla \cdot (n_z \mathbf{v}) = \nabla \cdot (D \nabla n_z) + \mathcal{I}_{z-1} n_{z-1} - (\mathcal{I}_z + \mathcal{R}_z) n_z + \mathcal{R}_{z+1} n_{z+1} + \mathcal{S}_z$$

- Thermal energy lost from plasma due to
  - Ionization
  - Line radiation
  - Bremsstrahlung radiation
  - Recombination radiation
- **Subcycled much faster than typical MHD time steps**

\*D.G. Whyte, et al., Proc. of the 24th Euro. Conf. on Controlled Fusion and Plasma Physics, Berchtesgaden, Germany, 1997, Vol. 21A, p. 1137.

# KPRAD Couples\* to the M3D-C1 Temperature Equation(s)

- **Two temperature equations (electron & all-ions)**

- Dilution cooling of ions and electrons
- Electrons lose energy to ionization and radiation
- Main ions cool on electrons

$$n_e \left[ \frac{\partial T_e}{\partial t} + \mathbf{v} \cdot \nabla T_e + (\Gamma - 1) T_e \nabla \cdot \mathbf{v} \right] + \sigma_e T_e = (\Gamma - 1) \left[ \eta J^2 - \nabla \cdot \mathbf{q}_e - \mathcal{P}_{rad} + Q_{ei} - \Pi_e : \nabla \mathbf{v} \right]$$

$$n_* \left[ \frac{\partial T_i}{\partial t} + \mathbf{v} \cdot \nabla T_i + (\Gamma - 1) T_i \nabla \cdot \mathbf{v} \right] + \sigma_* T_i = (\Gamma - 1) \left[ -\nabla \cdot \mathbf{q}_* - Q_{ei} - \Pi_* : \nabla \mathbf{v} + \frac{1}{2} \varpi_* v^2 \right]$$

- **Single temperature equation**

- Evolves sum over all species
- $T_e/T_i$  constant throughout time, implicitly assuming
  - Instantaneous thermal equilibration
  - Split of losses between species evolves as pressure ratio changes

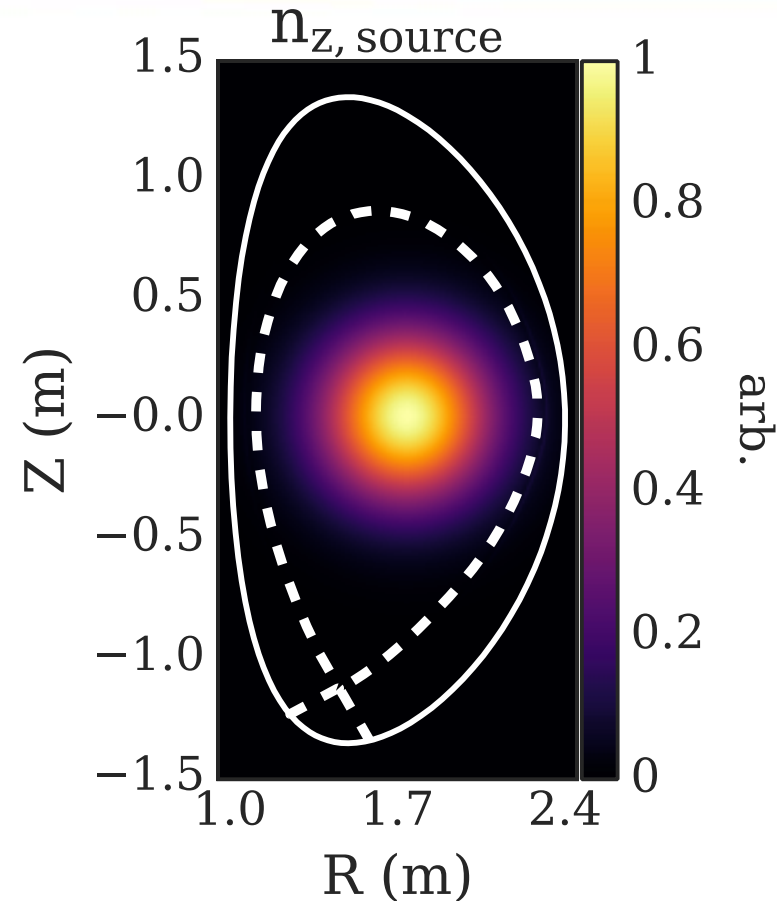
\*N.M. Ferraro et al. Nucl. Fusion 59 016001 (2019).

# Verification Benchmarks of NIMROD & M3D-C1



# Axisymmetric Benchmark Successful for Fast Impurity Injection in DIII-D Core

- **Four cases solved by both M3D-C1 and NIMROD\***
  - [Lyons et al., PPCF 61, 064001 \(2019\)](#)
  - Shown here: argon with Spitzer resistivity
- **Simulation setup**
  - DIII-D shot 137611 @ 1950 ms
  - 2D, nonlinear, single-fluid
  - Fixed boundary
- **Continuous neutral impurity deposition**
  - No impurities to start
  - Gaussian source
$$\frac{dn_z}{dt} = \nu \frac{R_0}{R} \exp \left[ -\frac{(R - R_0)^2 + (Z - Z_0)^2}{2\delta^2} \right]$$
  - Injection rate  $\sim 1$  mm Ne/Ar per ms

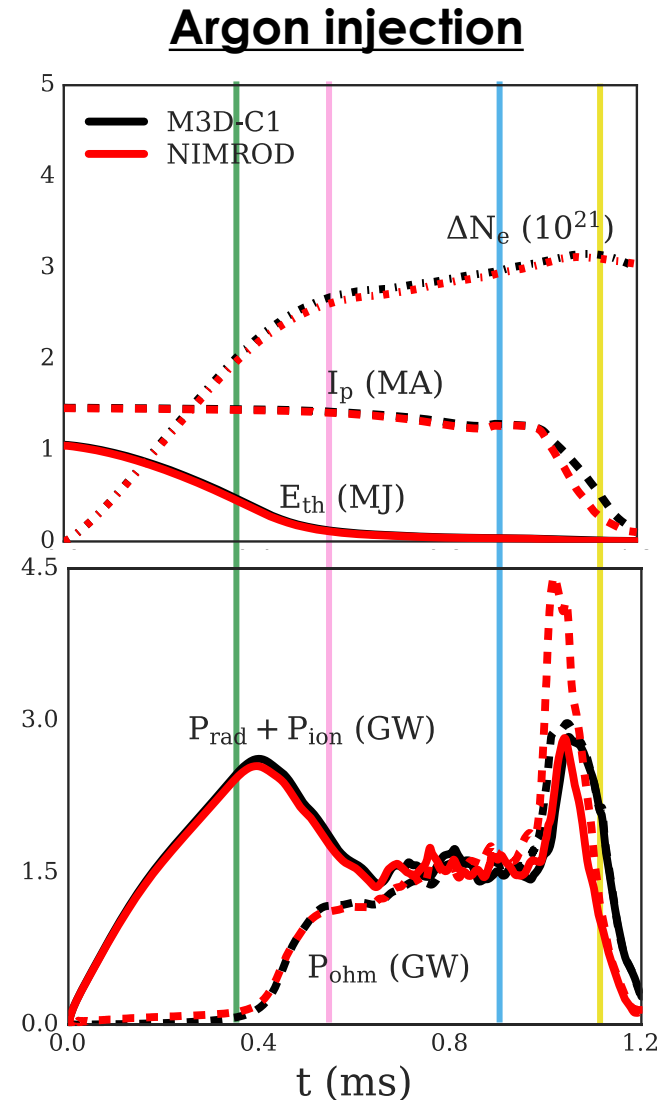


\*C. R. Sovinec et al., J. Comput. Phys. 195, 355 (2004).

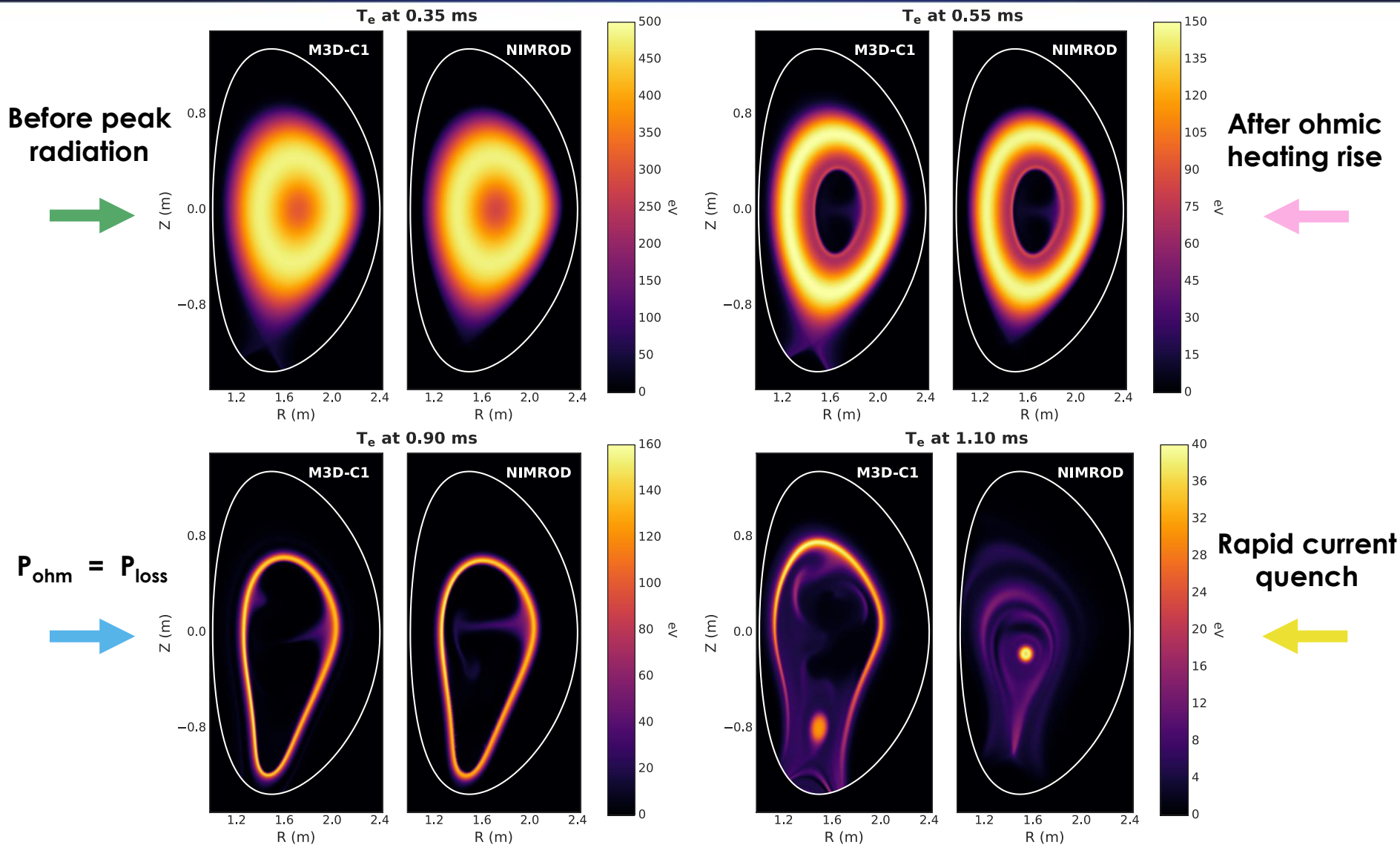
C. Sovinec & J. King, J. Comput. Phys. 229, 5803 (2010).

# Excellent Agreement Found Between Codes in 2D

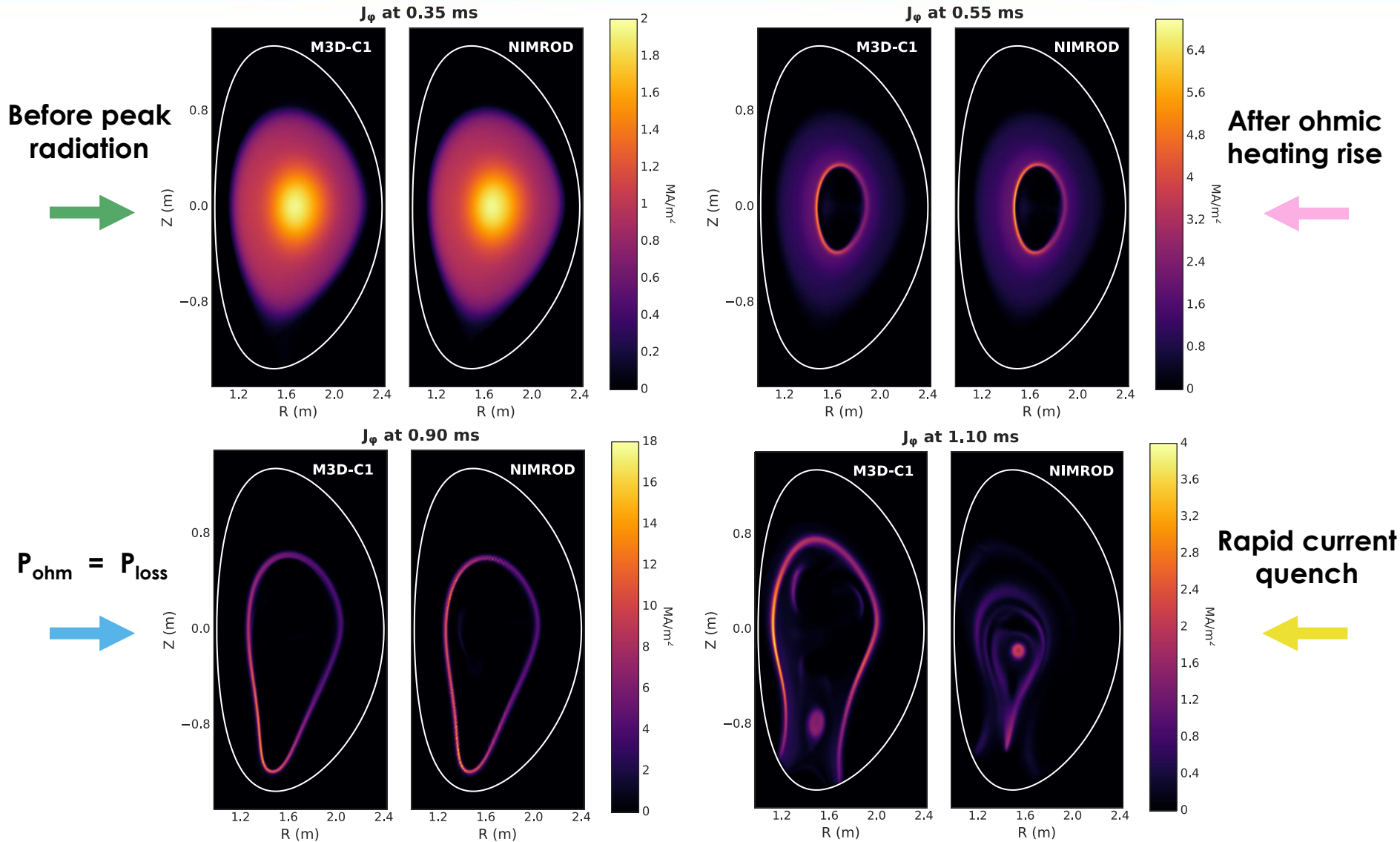
- Quantitative agreement during thermal quench (TQ)
- Qualitative agreement during current quench (CQ)
- Low temperature in core causes resistivity to rise
  - $P_{\text{ohm}}$  balances  $P_{\text{loss}}$
  - Current drops more rapidly
- Current quench caused by contact with boundary
- Peak loss power when temperature on-axis falls near-zero



# Impurities Induce Inside-Out Thermal Quench with Core Turbulence



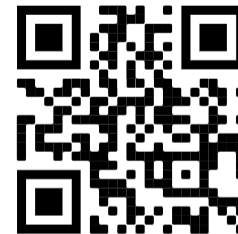
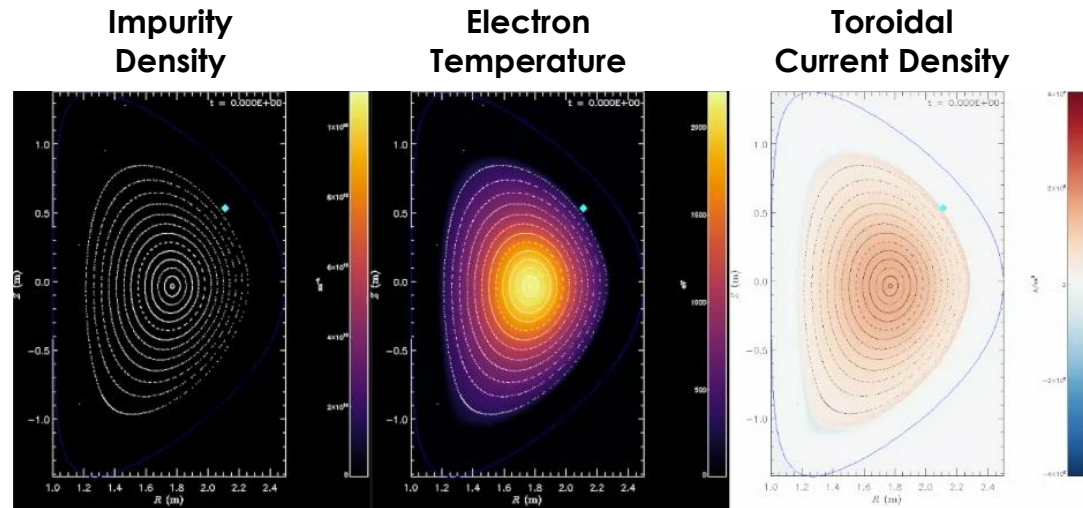
# Current Localizes to Thin, Expanding Shell that Contacts Domain Boundary



# 3D, Nonlinear Benchmark Between M3D-C1 & NIMROD for Realistic, Injected Pellet is Well-Underway

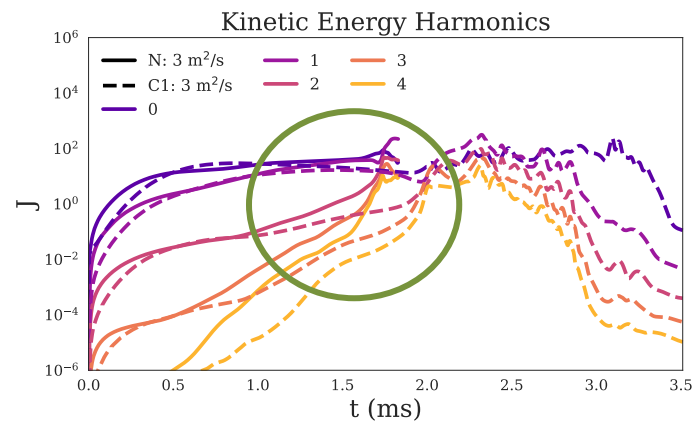
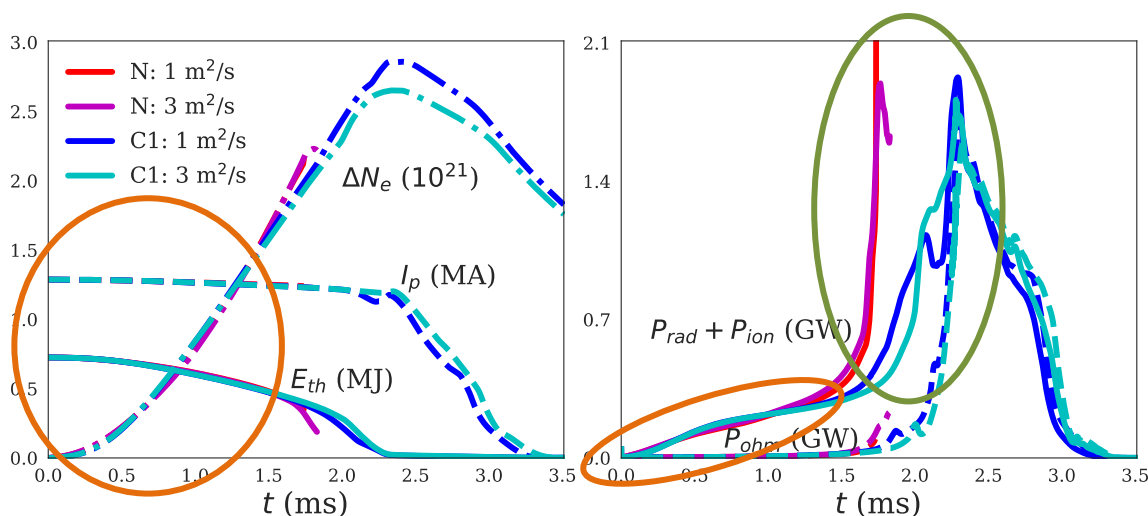
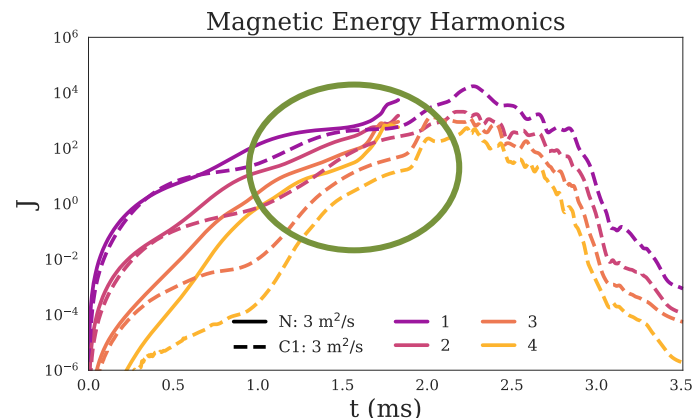
- **3D nonlinear MHD**
  - Fixed boundary
  - Single-temperature equation
- **Pellet/deposition parameters**
  - 3 mm radius, pure neon
  - 5 cm poloidal and 2.4 m toroidal half-width
  - 200 m/s with realistic trajectory
  - Ablation by local electron density and temperature according to model by Parks
- **Work has motivated code development and provided insight into SPI physics**

**M3D-C1 Modeling of DIII-D 160606 @ 2990 ms:**  
**0.7 MJ, 1.28 MA**



# M3D-C1 & NIMROD Differ in Timing of Instability Onset

- **Early, radiation driven thermal quench in good agreement**
- **NIMROD shows earlier spike in radiation, driven by earlier MHD instability onset**
- **M3D-C1 observes stabilization from density diffusivity**



# Difference in 3D Benchmark Possibly Caused by Flow Discrepancy due to M3D-C1 Boundary Condition

- Flow differs even before time traces diverge, especially in open-field-line region
- Caused by M3D-C1 implementation of normal/poloidal no-flow BC

- M3D-C1 uses potential formulation

$$\vec{u} = R^2 \nabla U \times \nabla \varphi + R^2 \omega \nabla \varphi + \frac{1}{R^2} \nabla_{\perp} \chi$$

- BCs should be:

- No poloidal:  $R \frac{\partial U}{\partial n} + \frac{1}{R^2} \frac{\partial \chi}{\partial \tau} = 0$

- No normal:  $-R \frac{\partial U}{\partial \tau} + \frac{1}{R^2} \frac{\partial \chi}{\partial n} = 0$

- Instead using

$$\frac{\partial U}{\partial n} = 0 \quad \text{and} \quad \chi = 0$$

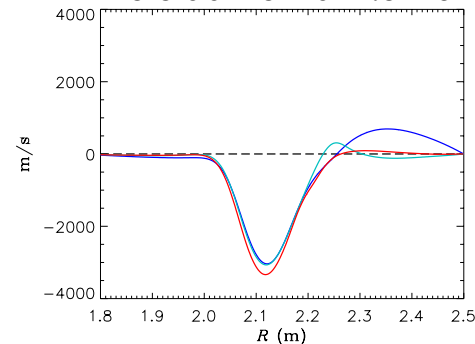
$$U = 0 \quad \text{and} \quad \frac{\partial \chi}{\partial n} = 0$$

which over-constrains solution

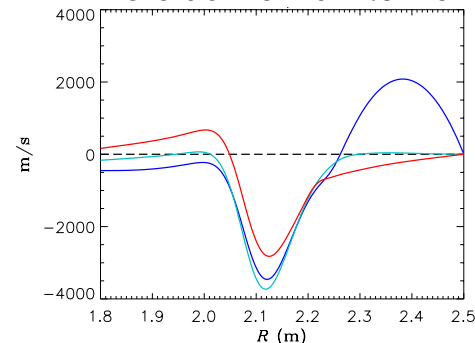
- **New BCs implemented in M3D-C1**

- Using only new no-poloidal gives better flow agreement, but does not change 3D benchmark results
- Maybe needs both, but that's currently numerically unstable

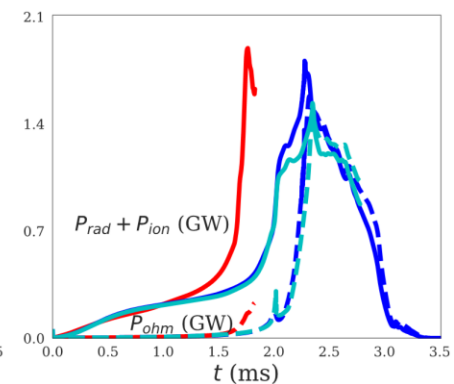
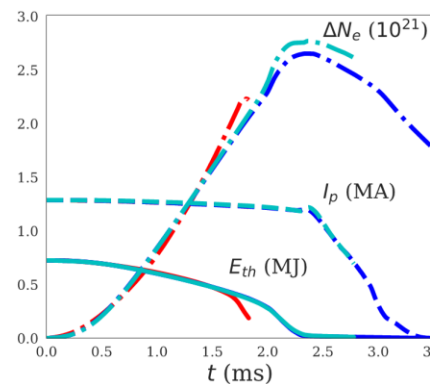
Poloidal flow at 1.0 ms



Toroidal flow at 1.0 ms



**NIMROD**  
**C1: Old no-pol.**  
**C1: New no-pol.**

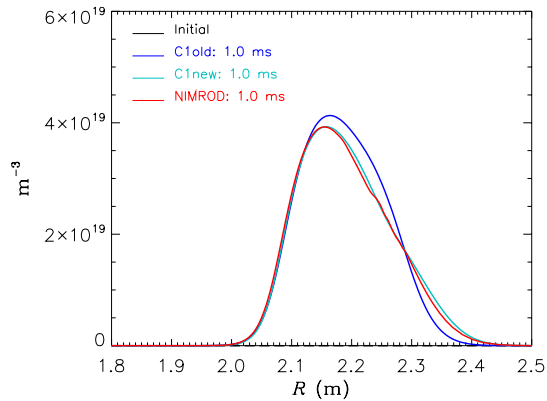




# Differences in Other Key Profiles Perhaps Hint at Another Cause?

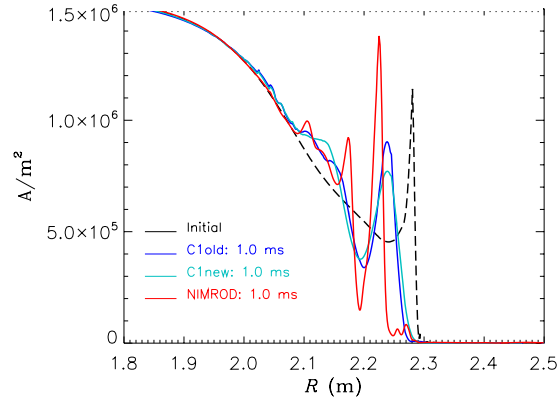
**NIMROD**  
C1: Old no-pol.  
C1: New no-pol.

### Impurity Density

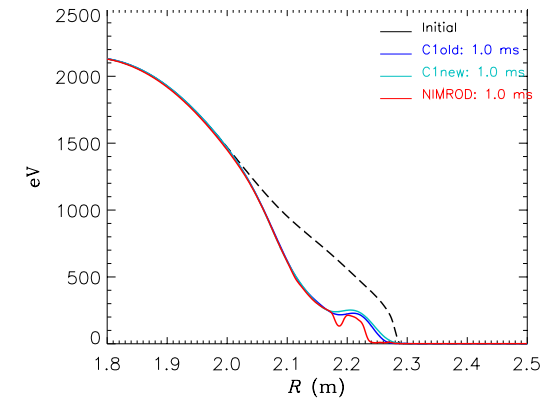


1.0 ms

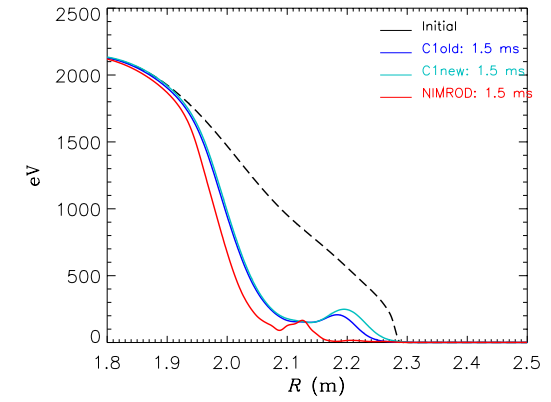
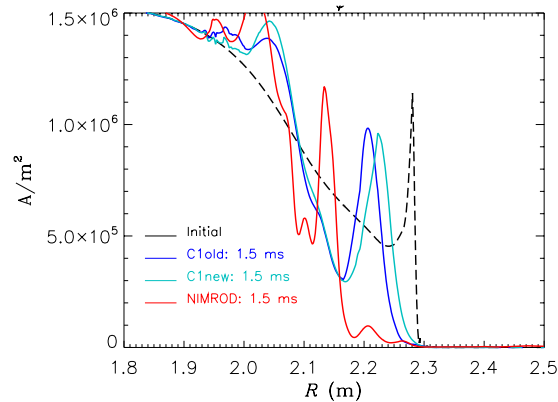
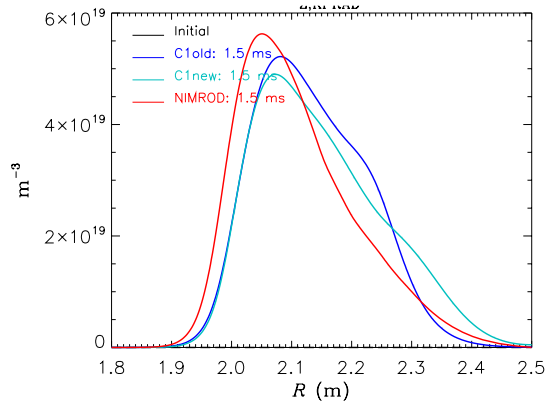
### Current Density



### Electron Temperature



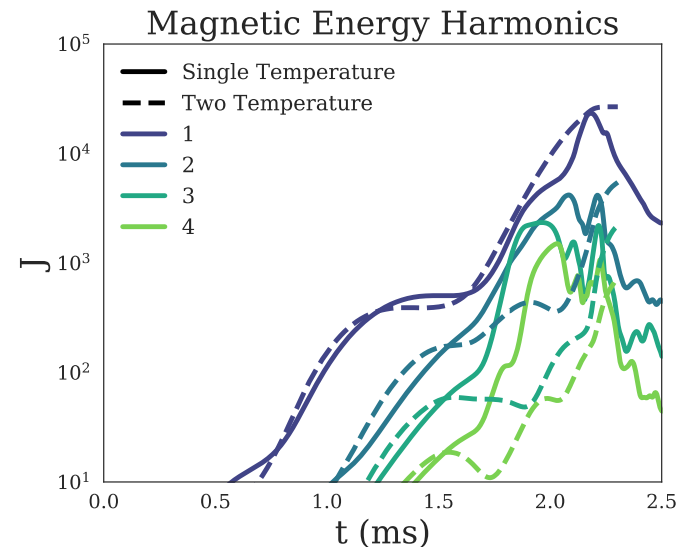
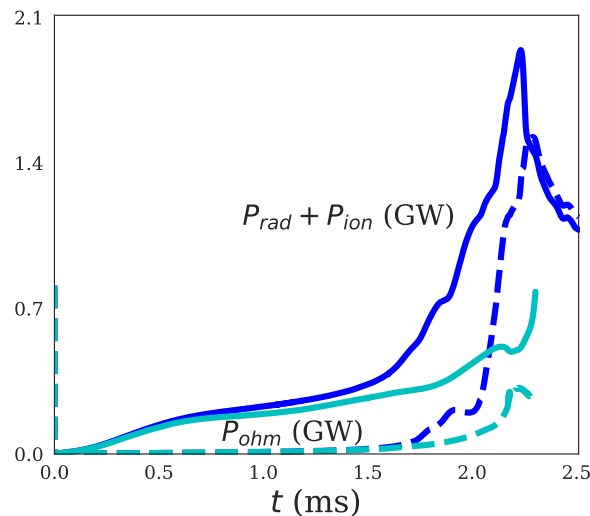
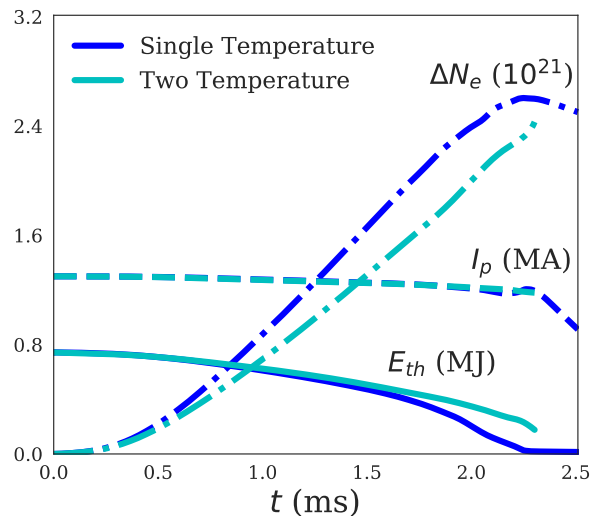
1.5 ms





# Two-Temperature Modeling Shows Delayed Thermal Quench

- **M3D-C1 benchmark case re-run with two-temperature model**
- **Early dynamics similar, but deviates as electrons cool faster than single-temperature model**
  - Less ablation and ionization
  - Slower thermal quench
  - Delayed instability
- **Single-temperature model may underpredict thermal-quench times and overpredict pellet assimilation**

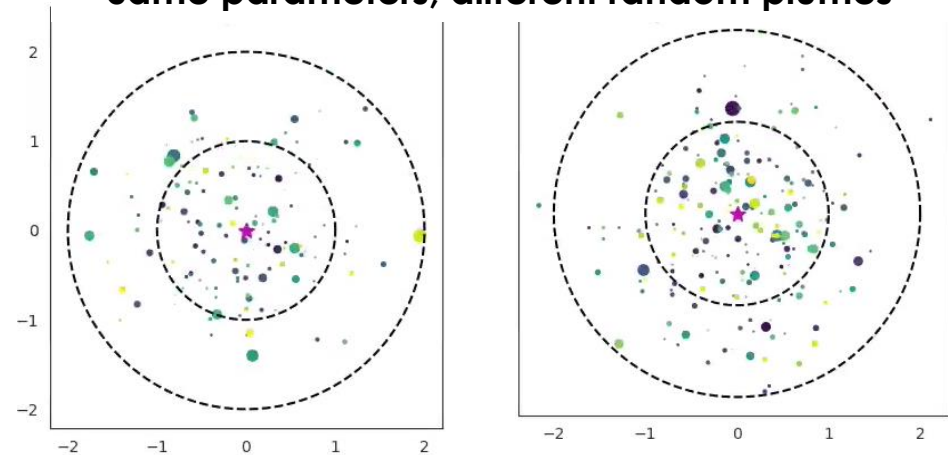


# SPI Plume Modeling in JET

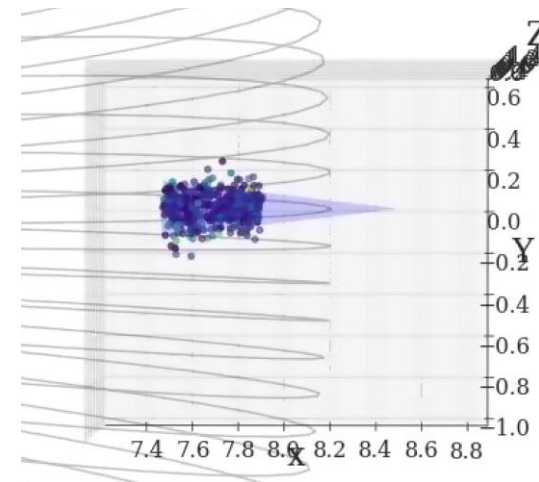
# M3D-C1 Multi-Fragment Modeling Uses Realistic Model for Shattered Plumes

- **Script created to generate shatter plumes**
  - Uniform fragments
  - Fracture-threshold theory  
[T.E. Gebhart et al. IEEE 48, 6 \(2019\)](#)
- **Distribution options**
  - Sunflower distribution
  - 2D uniform
  - Gaussian poloidal/toroidal spread
- **Easily generate random (but reproducible) plumes for different pellet size, speed, and composition**
- **Being used for reference plumes in JET & KSTAR modeling by M3D-C1, NIMROD, and JOEK**

Same parameters, different random plumes

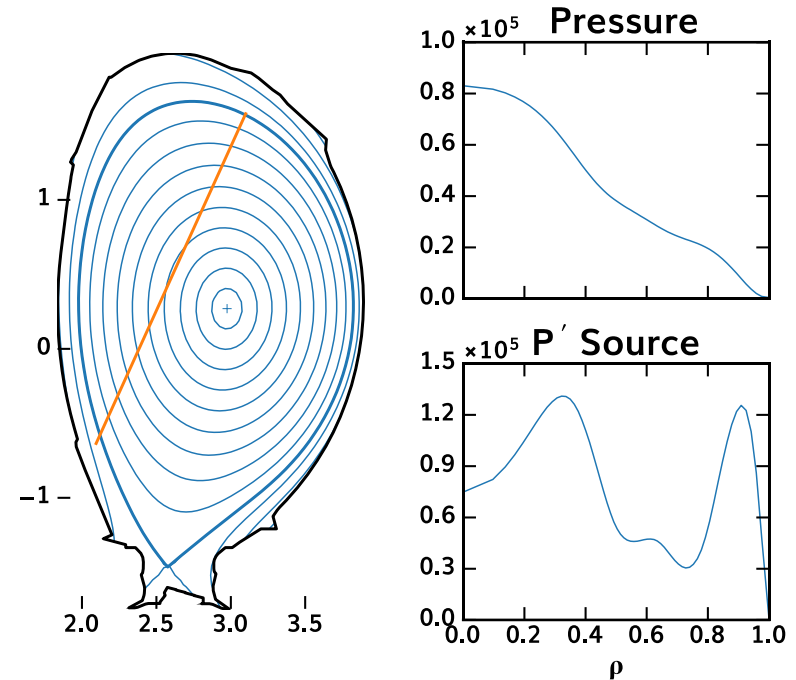


Spread in tokamak geometry



# M3D-C1 JET Modeling with Realistic Plumes Performed for JET Scenario 1

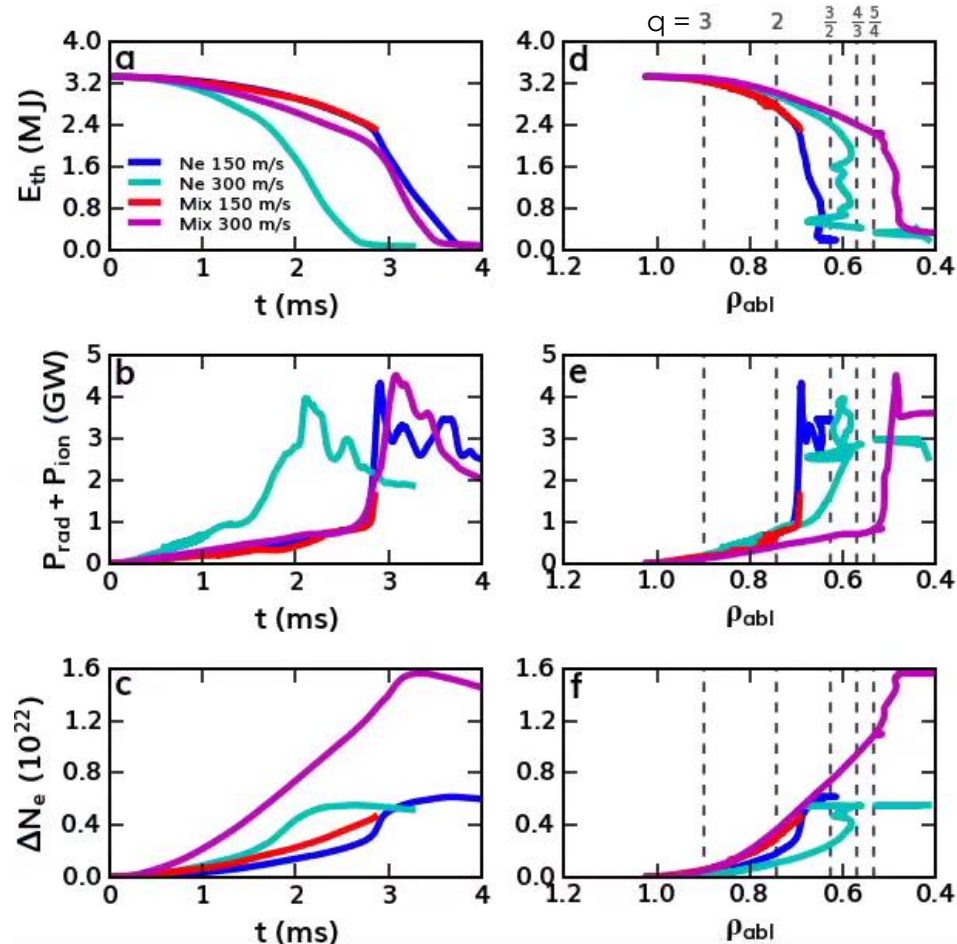
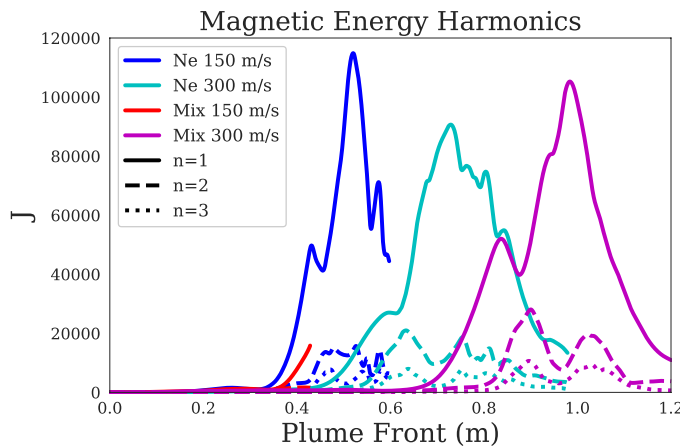
- Based on high-thermal-energy (Scenario 1) plasma with 8.1 mm cylindrical pellet
- Equilibria reconstructed with kinetic profiles acquired for recent experiment
- Two realistic pellets travel along nominal trajectory
  - Pure Neon
    - 30 1.71-mm shards
    - 150 m/s
  - 95% D:
    - 85 1.21-mm shards
    - 300 m/s
  - Uniform shard size computed from ablation-average of cloud
- Also consider same plumes but swapped speeds



**JET 95707**  
 **$I_p = 2.4$  MA**  
 **$W_{th} = 3.4$  MJ**  
**(Scenario 1 High  $W_{th}$ )**

# JET Modeling Shows Competition Between Rate of Travel and Rate of Radiative Dissipation

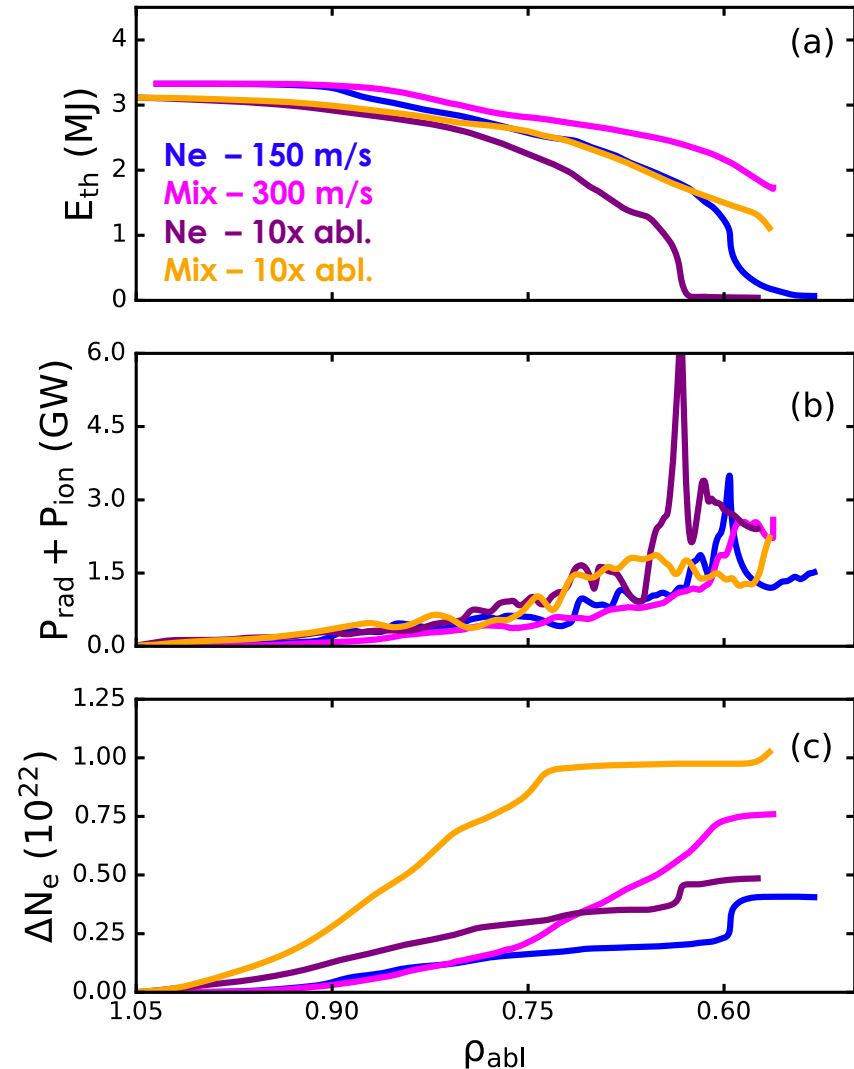
- All plumes show similar peak radiated power
- Dynamics versus time
  - Fast neon has earliest TQ
  - Others have similar TQ times
- Dynamics versus penetration depth
  - Slow: both travel same to same depth – radiation dominates
  - Fast: mixed pellet travels deeper – doesn't radiate fast enough to induce instability
  - Deeper penetration leads to increased mode coupling



shard position,  
weighted by ablation rate

# NIMROD JET Modeling With Same Realistic Plumes Also Underway

- **Realistic plumes**
  - Faster, mixed pellet penetrates further, as in M3D-C1
  - Generally deeper penetration than M3D-C1, possibly due to impurity deposition behind pellet?
- **Simulations with increased ablation rate show acceleration of thermal quench**
  - Longer period of similar decay perhaps shows increased dominance of radiative dissipation
  - Comparison challenging due to use of different equilibria



# Future M3D-C1 Disruption Mitigation Work

- **M3D-C1 & NIMROD 3D benchmark**
  - Continue convergence studies
    - Poloidal & toroidal resolution
    - Time step
    - Diffusivities
  - Need to determine metrics for success
    - Strong nonlinearity makes exact agreement difficult
    - Chaotic evolution: small discrepancies early cause exponential deviation
    - Perhaps use physically relevant quantities, e.g., assimilation fraction, radiation fraction/peaking, TQ time
- **Validate JET modeling against experimental results**
- **Perform & validate KSTAR modeling of multiple toroidal injection**
- **Predictive modeling for ITER SPI**